

Probing the Electronic Structure of Peptide Bonds Using Methyl Groups[†]

David F. Plusquellic*

Optical Technology Division, National Institute of Standards and Technology, Gaithersburg, Maryland 20899

David W. Pratt

Department of Chemistry, University of Pittsburgh, Pittsburgh, Pennsylvania 15260

Received: January 31, 2007; In Final Form: May 17, 2007

The observed V_3 torsional barriers measured by microwave spectroscopy for nine methyl groups attached α to peptide bond linkages in five gas-phase biomimetics have been found to differ considerably from one molecule to the next and even depend on the position of substitution, being sensitive to structural changes at the other end of the peptide bond. In the search for an explanation for these results, ab initio calculations have been performed at the HF/6-311++G(d,p) level of theory and interpreted in terms of the natural bond orbitals and resonance structures of the peptide bond. These calculations reveal that resonance delocalization in peptide bonds is influenced by methyl conformation through the coupling of vicinal σ to σ^* orbital interactions with the n to π^* . Thus, CN double-bond character increases (and CO double-bond character decreases) as the methyl group is rotated from the syn to the anti position. A quasilinear correlation exists between the barriers to internal rotation of attached methyl groups and the relative importance of the two principal resonance structures that contribute to the peptide bond.

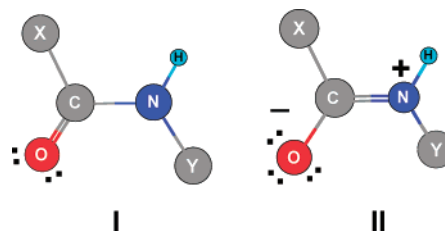
I. Introduction

Pauling¹ was the first to suggest that the secondary structural motifs we now know as α -helices and β -sheets have their origins in a planar peptide bond, arising from the two Lewis structures **I** and **II**; see Chart 1. Implicit to the dipolar form of **II** is a large delocalization of charge from the nitrogen lone pair to the carbonyl oxygen with an accompanying increase/decrease in the C=O/C–N bond lengths. Empirical evidence in support of this simple resonance picture is now extensive. Correlations have been drawn from structural data on numerous model peptides. For example, the observed C–N bond lengths,^{2–5} the planarity of the C(O)NH fragment,^{2,4} and the torsional rigidity of the C–N bond⁶ are all consistent with this model. Thus, the barriers to internal rotation about the C–N bond are direct measures of the relative importance of the two Lewis structures, higher barriers resulting from larger contributions from structure **II**.

On a larger scale, additional evidence comes from the compiled databases of high-resolution crystal structures of peptides⁷ and proteins⁸ where strong negative correlations have been shown to exist between the C=O and C–N bond lengths. Recently, the relative importance of Lewis structures **I** and **II** has been shown to strongly influence the coil-to-helix folding rates in molecular dynamics simulations.⁹ The Pauling model is now generally accepted within the framework of valence bond theory and deeply entrained in the introductory material of many biochemistry textbooks on protein structure. Other resonance forms are possible^{10–15} but are generally found to be of much less importance.

Here, we show that another degree of freedom, the torsional motion of a methyl group attached α to a peptide linkage, also

CHART 1



reports on (and influences) the relative importance of structures **I** and **II**. Rotations about the C–X and N–Y bonds correspond to changes in the Ramachandran angles ψ and φ , respectively.¹⁶ Recent measurements of the V_3 torsional barriers of methyl groups in a number of biomimetic systems by gas-phase Fourier transform microwave (FTMW) techniques have provided the stimulus for the current investigation. In what follows, we describe these results, we show that they can be readily accounted for by ab initio calculations, and then we use the results of the calculations to establish a heretofore unrecognized link between the experimentally measured barriers to methyl group rotation and the relative importance of the different resonance structures contributing to the peptide bond.

II. Theoretical Methods

Electronic structure calculations were carried out at the HF/6-311++G(d,p) level of theory using Gaussian 03.¹⁷ Methyl torsional barriers were calculated by first constructing a z -matrix representation in which the torsional coordinate was defined by a single dihedral angle between the in-plane C–H bond of the methyl group and the C–N peptide bond. The dihedral angles of the two out-of-plane H atoms were defined relative to this in-plane C–H bond. For nonplanar structures, the bond most nearly in-plane was chosen as the reference. Initial top-

[†] Part of the “Roger E. Miller Memorial Issue”.

* To whom correspondence should be addressed. E-mail: david.plusquellic@nist.gov.

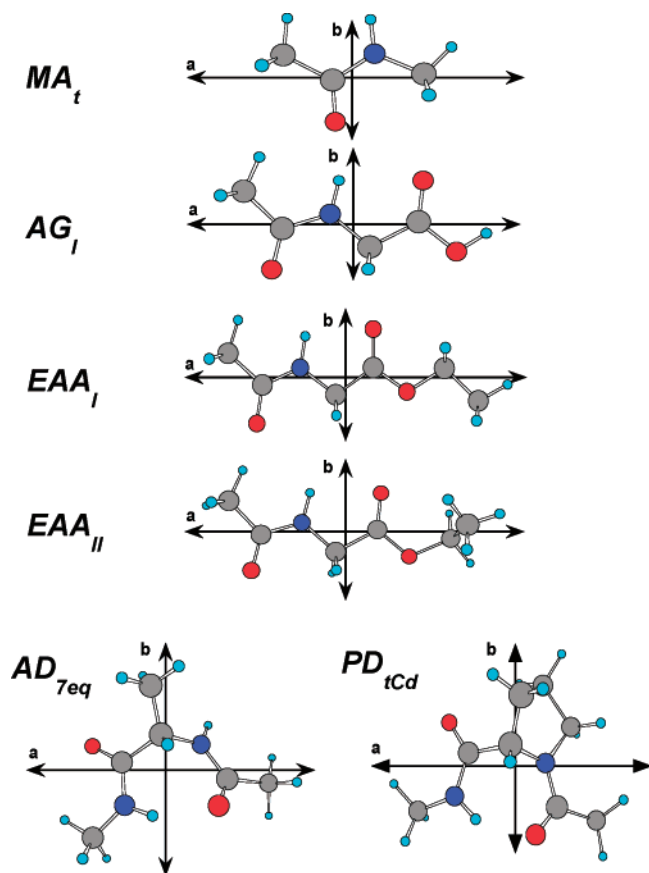


Figure 1. The six different molecules and configurations studied having one or more methyl tops attached to one or more peptide bonds.

of-the-barrier or saddle point structures were defined by adding 180° to the methyl torsional coordinate. The V_3 barriers reported here are the energy differences between the fully optimized saddle point and the equilibrium structures. Therefore, constrained geometry optimizations using a symmetry adapted torsional coordinate were not necessary.¹⁸ Results from fully relaxed potential energy surface scans were performed at fixed values of the dihedral angles, typically in 15° increments and used for illustrative purposes only.

The orbital character and energetics of the peptide bond and their dependence on the methyl torsional coordinate(s) were investigated using the natural bond orbital (NBO) formalism developed by Weinhold and co-workers.^{19–22} The NBO treatment partitions the wave function into a set of localized bonding and lone pair orbitals corresponding to the formal Lewis structure of the molecule and a set of antibonding and Rydberg-like (non-Lewis) NBOs necessary to fully span the basis and to characterize the delocalization of charge from the Lewis-like NBOs.

Two types of interactions may be rigorously separated in this basis within the theoretical framework of a one-particle density matrix.¹⁹ The first type relates to the localized interactions of the NBOs of an idealized Lewis structure. These interactions are steric in nature and include both electrostatic and exchange repulsion forces. The second type of interaction arises from the delocalization of the Lewis-like NBOs into empty antibonding and Rydberg-like (non-Lewis) orbitals. The magnitudes of the stabilization energies arising from these donor–acceptor interactions are computed in two different ways in the NBO suite.²² The total energy from delocalization is obtained rigorously by first calculating the self-consistent field (SCF) energy of the idealized system having all antibonding and Rydberg-like orbitals removed and then comparing this energy with the exact

TABLE 1: Observed V_3 Barriers Determined from Gas-Phase FTMW Studies of the Selected Peptide Mimetics Shown in Figure 1

label	structure	symmetry	V_3 barrier (cm ⁻¹) ^a	ref
Me _C Groups				
MA _t	CH ₃ –[CONH]–CH ₃	C _s	+73(2)	23
AG _I	CH ₃ –[CONH]–CH ₂ –C(O)OH	C _s	+57(2)	24
EAA _I	CH ₃ –[CONH]–CH ₂ –C(O)OC ₂ H ₅	C _s	+66(2)	25
EAA _{II}	CH ₃ –[CONH]–CH ₂ –C(O)OC ₂ H ₅	C ₁	+66(2)	25
AD _{7eq}	CH ₃ –[CONH]–CHCH ₃ –[CONH]–CH ₃	C ₁	+98(2)	26
PD _{tCd}	CH ₃ –[CON]–CHC ₃ H ₆ –[CONH]–CH ₃	C ₁	+333(5)	27
Me _N Groups				
MA _t	CH ₃ –[NHCO]–CH ₃	C _s	+79(2)	23
AD _{7eq}	CH ₃ –[NHCO]–CHCH ₃ –[CONH]–CH ₃	C ₁	+84(2)	26
PD _{tCd}	CH ₃ –[NHCO]–CHC ₃ H ₆ –[CON]–CH ₃	C ₁	+84(2)	27

^a The expanded uncertainties shown in parentheses are type B with coverage factor $k = 1$ or 1 standard deviation.

SCF energy. Approximate stabilization energies from delocalization also are given for specific bond and antibond or Rydberg orbital pairs using second-order perturbation theory.

The resonance character of the peptide bonds was investigated using natural resonance theory (NRT)²¹ which takes the calculated charge density and recasts it in terms of a set of idealized resonance or Lewis structures. This is done by first expanding the one-electron reduced density operator in terms of a resonance hybrid of density operators. The resonance weights are obtained variationally to give the best description of the charge density in terms of the reference Lewis structures.

III. Microwave and *ab Initio* Results

The molecules considered in this study are shown in Figure 1. Each of the structures contains one or more methyl groups attached to one or more peptide bonds and includes (i) the trans form of *N*-methyl-acetamide (MA_t),²³ (ii) the planar form of *N*-acetyl-glycine (AG_I),²⁴ (iii) the planar and nonplanar forms of ethylacetamidoacetate (EAA_I and EAA_{II}),²⁵ (iv) the C₇^{eq} form of alanine dipeptide (AD_{7eq}),²⁶ and (v) the trans down-puckered ring form of proline dipeptide (PD_{tCd}).²⁷ For these five model systems, torsional barriers have been determined for all nine of the methyl groups attached to the N- and C-termini of the peptide bonds. These determinations have been made from analyses of the rotational structure built on the two lowest torsional sublevels of *A* and *E* symmetry, both of which remain populated in a free jet expansion at 2 K regardless of the energy difference between them. In most cases, only the leading term, V_3 , of the Fourier expansion of the torsional potential given in eq 1 has been determined,

$$E = \frac{V_3}{2}(1 - \cos 3\theta) + \frac{V_6}{2}(1 - \cos 6\theta) + \dots + \frac{V_{12}}{4}(\sin 3\theta \cos 3\theta) + \dots \quad (1)$$

where θ is the torsional coordinate. The V_6 terms were shown to impact the torsional barriers for carbonyl methyl groups attached to peptide bonds²⁸ by less than 15%, and the latter terms are known to be important only for coupled rotor systems.²³ In some cases, different formalisms have been used to extract V_3 values from the data; in those few cases where different methods were used, similar values of V_3 were obtained.^{25,28}

The experimentally determined V_3 torsional barriers of the nine peptide bond methyl rotors are listed in Table 1. The methyl groups fall into two classes; six are attached to the carbonyl

TABLE 2: Lewis and Non-Lewis Energy Differences Calculated at the HF/6-311++G(d,p) Level of Theory that Contribute to the Methyl Torsional Barriers^a

	V_3^E	kcal/mol		cm^{-1}	
		Lewis	non-Lewis	V_3 calcd	V_3 exptl
Me _C Groups					
AG _I	anti	-1.86	+2.02	+54	+57(2)
EAA _I	anti	-1.90	+2.07	+59	+66(2)
EAA _{II}	anti	-1.89	+2.06	+60	+66(2)
MA _t	anti	-1.88	+2.07	+70	+73(2)
AD _{7eq}	anti	-2.85	+3.04	+67	+98(2)
PD _{tCd}	syn	+6.33	-5.54	+278	+333(5)
Me _N Groups					
MA _t	syn	+1.88	-1.52	+126	+79(2)
AD _{7eq}	syn	+2.47	-1.98	+170	+84(2)
PD _{tCd}	syn	+4.24	-3.75	+171	+84(2)

The labels anti or syn designate the minimum energy orientation of the in-plane C–H bond relative to the C=O or N–H bonds.

end (Me_C) of the peptide bond and three are attached to the amide end (Me_N). In general, the torsional barriers are small, ranging between 0.2 and 1 kcal/mol (1 kcal/mol \approx 350 cm^{-1}).²⁹ Notice, however, that while the local environments of the methyl groups within each class are nearly identical, the rotational barriers are sensitive to structural differences at the other end of the peptide bond, those of the Me_C more so than those of Me_N. The Me_C group of PD_{tCd} is the only exception. In a related paper, we show that steric interactions between this group and the prolyl ring hydrogen atoms dominate the energetics of the torsional barrier.²⁷

Table 2 lists the ab initio values of the torsional barriers and associated conformational minima of each methyl group. The relative magnitudes of the predicted barriers are in good agreement with observations, although the Me_C barriers are slightly underestimated and the Me_N barriers are somewhat overestimated. The ab initio results predict that the in-plane C–H bond of the carbonyl methyl groups prefers a configuration anti to the carbonyl group, in contrast to the syn minima reported for other carbonyl systems.³⁰ Similar geometry optimizations of the amide methyl group reveal a syn preference for the in-plane C–H bond relative to the N–H bond. (These same equilibrium conformations are also predicted at the MP2/6-311G(d,p) and MP2/cc-pVTZ levels. However, in some cases, the equilibrium position of the amide methyl group is reversed at the B3LYP/6-311++G(d,p) level. See Tables 5S–12S in Supporting Information).²⁸ Many empirical packages³¹ (including CHARMM which is optimized for protein structure)³² predict just the opposite for one or both classes of methyl groups, i.e., a syn–anti equilibrium configuration of the carbonyl and amide methyl groups, respectively.

IV. Natural Bond Orbital Analysis

The internal rotation barrier in CH₃NH₂ is on the order of 1000 cm^{-1} .³³ It is thus apparent that the comparatively small barriers observed in the gas-phase biomimetics arise from a near cancellation of much larger effects. In the search for an explanation of this behavior, the NBOs were calculated for both the equilibrium and saddle point geometries using the NBO program suite.²² The Lewis (LE) and non-Lewis (NLE) energy contributions were obtained using the orbital deletion option as described above and are reported in Table 2 as the differences between the saddle point and equilibrium structures in units of kcal/mol. Positive values indicate a preference for the equilibrium form, and negative values indicate a preference for the saddle point form. Their sum gives the magnitude of the

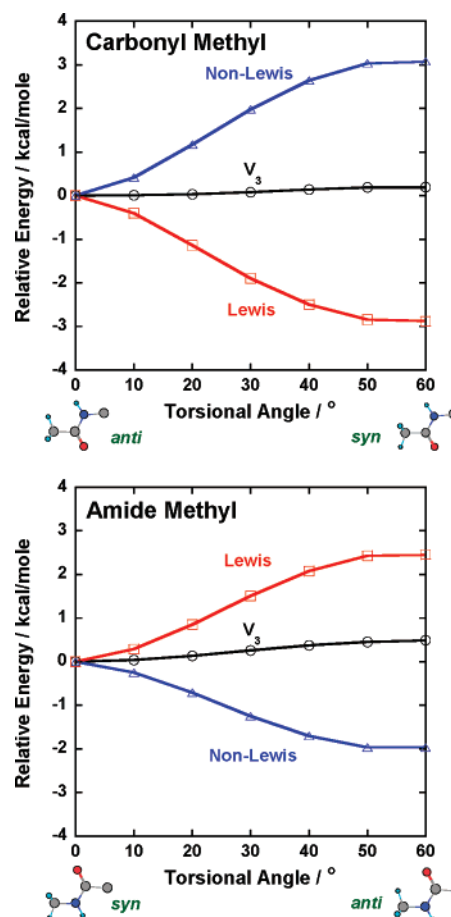


Figure 2. Methyl torsional coordinate dependence of the Lewis and non-Lewis energies of the Me_C (upper panel) and Me_N (lower panel) rotors of alanine dipeptide (AD_{7eq}). The torsional potential energy surfaces of the methyl rotor result from the sum of these two contributions and are shown as the center curve in each panel.

calculated barrier and is given in Table 2 under V_3 (calcd) in units of cm^{-1} . Between these limiting cases, the LE and NLE vary smoothly as a function of torsional angle. These results are shown in Figure 2 together with the fully relaxed potential energy surface data for both rotors of AD_{7eq}.

Notice, first, that in all cases the NLEs from delocalization are large and comparable to the LE of 2–6 kcal/mol. The calculated V_3 barriers represent less than $1/10$ of these energies. As clearly evident from Figure 2, the torsional barriers are a result of a delicate balance between these two opposing contributions. For the Me_C rotors, the NLEs are positive for the anti configuration and, since they are dominant, the anti form is the V_3 minimum energy structure. PD_{tCd} is the only exception. In contrast, LEs are more important for the Me_N groups and positive when the methyl group adopts a syn configuration.

Given the opposing nature of the forces responsible for the low torsional barriers and the remarkable similarities exhibited across this series, we have examined in some detail the principal contributions to the LEs and the NLEs. The details of this analysis may be found in the Supporting Information; we summarize the principal findings below.

The contributions to the Lewis energies may be broken down into a set of NBO interactions that are vicinal (or adjacent) to the methyl group orbitals and a remote set that includes all others. For the Me_C rotors, we find that the energy sum over all of the vicinal NBOs is near zero. Thus, the LE difference is a result of the remote orbital class. This trend gives us a qualitative explanation for the increased sensitivity of the Me_C

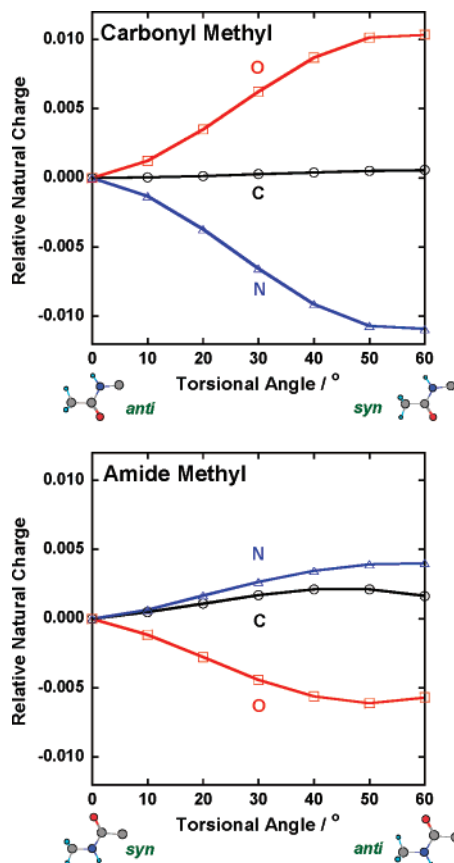


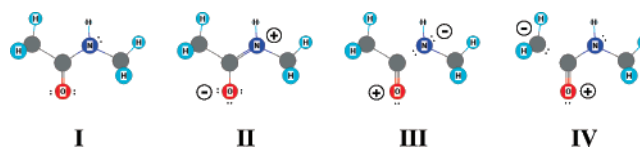
Figure 3. Methyl torsional coordinate dependence of the natural charges associated with the O atom and C- and N-fragments of the peptide bond. The charges are plotted relative to the equilibrium charges of the Me_C (upper panel) and Me_N (lower panel) rotors of alanine dipeptide (AD_{7eq}).

barriers (cf. Table 1) to the group attached at the other end of the peptide bond. In contrast, the sum of the local steric energies remains important for the amide methyl rotors while there is a near cancellation of the remote interactions. This provides a basis for understanding the syn preferences predicted for the Me_N rotors versus the anti minima found for the Me_C groups.

The principal components of the NLE may be identified from examination of the second-order energies given for each pairwise NBO interaction. We find that for both the Me_C and Me_N rotors, the direct interaction energies with the methyl group orbitals tend to cancel and that the majority of the NLE difference arises from the $n_N \rightarrow \pi^*_{C=O}$ delocalization which is an indirect consequence of the methyl torsional motion. The large impact of these indirect interactions has an origin in the absolute NLEs of ≈ 100 kcal/mol for the $n_N \rightarrow \pi^*_{C=O}$ delocalization compared to the much smaller NLEs of 5–10 kcal/mol associated with the methyl NBOs.

Further insight into the $n_N \rightarrow \pi^*_{C=O}$ delocalization accompanying methyl torsional motion comes from shifts in charge density between the O, N, and C fragments of the peptide bond. The torsional dependence of these shifts is reflected by the relative natural charges shown in the upper and lower panels of Figure 3 for the Me_C and Me_N groups of AD_{7eq}, respectively. In the top panel, the oxygen atom becomes more positively charged and the N fragment becomes more negatively charged upon rotation of the Me_C group to the saddle point region. Little change occurs on the C fragment. In contrast, Me_N rotation to the saddle point region causes an increase in the relative electron charge density on oxygen that is offset by decreasing values on the N and C fragments. Table 4S gives a summary of the

TABLE 3: Resonance Weights of the Principal Lewis Structures of MA₁ Calculated at HF/6-311++G(d,p) for the Equilibrium and Saddle Point Geometries of the Carbonyl (Me_C) and Amide Methyl (Me_N) Groups



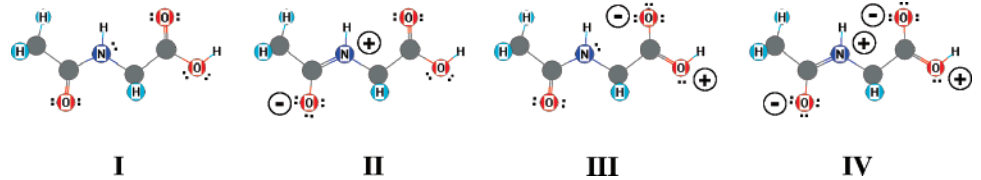
Lewis structure	natural resonance weights (%)		
	V_3^E	Me _C ($V_3^S - V_3^E$)	Me _N ($V_3^S - V_3^E$)
I	62.39	+1.16	-0.62
II	27.88	-1.13	+0.47
III	2.17	-0.07	+0.04
IV	1.75	+0.03	-0.02
Σ	94.19	-0.01	-0.13
I	67.93	+1.36	-0.54
II	32.07	-1.36	+0.54
Σ	100.0	+0.0	+0.0

results for the other seven rotors illustrating a consistent behavior observed across the series.

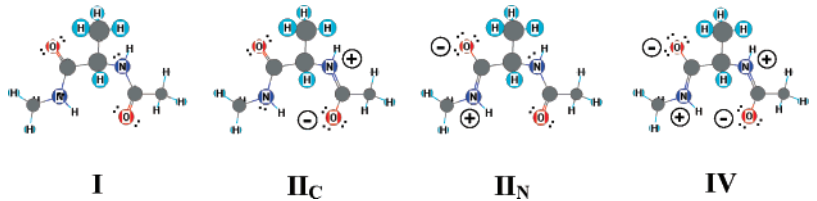
V. Natural Resonance Weights

We finally explore the connection between the observed torsional barriers and the resonance character of the peptide bonds. We begin with the simplest molecule, MA₁, having one peptide bond. At the HF/6-311++G(d,p) level of theory, NRT²¹ identifies the four leading structures shown in Table 3. The resonance weights obtained from variational fits are given for the equilibrium configurations of the Me_C and Me_N groups, and the weight changes are specified relative to the top of the barrier. The most prominent forms are Lewis structures **I** and **II** appearing in the ratio of 2:1 and together accounting for more than 90% of the weight. The saddle point regions of the methyl groups affect sizable changes in the weights of **I** and **II**, amounting to more than a 1% increase in **I** for Me_C and an approximately 0.5% decrease in **I** for Me_N. Conversely, little change occurs in the weights of **III** and **IV** or in any of the remaining 41 secondary structures. Given the small contributions from these higher energy resonance forms, calculations were performed with a detection threshold of 50 kcal/mol to eliminate all forms except **I** and **II**. The weights that now sum to 100% are given in the lower part of Table 3. The predicted changes from the truncated fit are similar to those above illustrating that charge density shifts accompanying methyl torsional motion are principally local to the peptide bond.

The results from a similar analysis of AG₁ are reported in Table 4. The leading four structures represent more than 80% of the total electron density. Again, NRT identifies Lewis forms **I** and **II** as the principal reference structures. However, the third and fourth structures gain in importance relative to those of MA₁ and are similar to **I** and **II** except for an ionic resonance on the carboxylic acid group. This reduces the combined weight of **I** and **II** to $\approx 75\%$. Interestingly, the absolute magnitudes of the weights of **III** and **IV** as well as the changes scale in proportion to those of the parent Lewis structures, **I** and **II**, respectively, even though these alternate resonance structures of the acid group are on the other side of the α carbon. The results given in the right-most columns of the table from calculations that include a detection threshold of 50 kcal/mol suggest an additive effect of these differences. Like the Me_C group of MA₁, the relative importance of **I** increases by more than 1% in the saddle point region.

TABLE 4: Resonance Weights of the Principal Lewis Structures of AG_I Calculated at HF/6-311++G(d,p) for the Equilibrium and Saddle Point Geometries of the Carbonyl (Me_C) Group


Lewis structure	natural resonance weights (%)			
	full expansion		partial expansion	
	V_3^E	$V_3^S - V_3^E$	V_3^E	$V_3^S - V_3^E$
I	52.28	+0.91	76.32	+1.12
II	20.94	-0.89	23.68	-1.12
III	5.10	+0.09		
IV	2.24	-0.09		
Σ	80.54	+0.02	100.0	+0.0

TABLE 5: Resonance Weights of the Principal Lewis Structures of AD_{7eq} and PD_{ICd} (Structure Not Shown) Calculated at HF/6-311++G(d,p) for the Equilibrium and Saddle Point Geometries of the Carbonyl (Me_C) and Amide Methyl (Me_N) Groups


Lewis structure	natural resonance weights (%)					
	V_3^E		$\text{Me}_C (V_3^S - V_3^E)$		$\text{Me}_N (V_3^S - V_3^E)$	
	AD _{7eq}	PD _{ICd}	AD _{7eq}	PD _{ICd}	AD _{7eq}	PD _{ICd}
I	35.47	33.27	+1.18	-1.17	-0.51	-0.23
II_C	18.09	15.95	-1.04	+0.91	-0.33	-0.36
II_N	17.32	16.19	+0.39	-0.44	+0.43	+0.31
IV	7.69	7.67	-0.54	+0.52	+0.17	+0.09
Σ	78.57	73.08	-0.01	-0.18	-0.24	-0.19
I	48.02	47.84	+2.09	-2.28	-0.76	-0.77
II_C	26.70	26.03	-2.05	+2.22	-0.04	+0.02
II_N	25.28	26.13	-0.04	+0.06	+0.80	+0.75
Σ	100.0	100.0	0.0	0.0	0.0	0.0

The leading structures, resonance weights, and changes predicted for the two conformations of EAA are similar to those of AG_I (see Table 5S). These similarities might be expected given that the structural and conformational differences between AG_I and EAA_I or EAA_{II} occur more than three atoms away from the peptide bond. Like AG_I, the proportional scaling of the weights and changes of Lewis forms **I–IV** in each conformer suggest some electronic communication across the α carbons. Furthermore, the slight increase in the relative importance of structure **II** in EAA_I and EAA_{II} compared to AG_I may explain the somewhat larger NLE contribution of 0.04 kcal/mol (Table 2). It is further satisfying to see that the nonplanarity of conformer EAA_{II} has no significant influence on the results of this analysis.

The resonance structures of AD_{7eq} and PD_{ICd} represent two examples of the increased importance of alternate resonance structures associated with additional peptide bonds. The four leading resonance structures of both molecules are shown in Table 5 and now consist entirely of Lewis structures **I** and **II** on one or both of the peptide bonds. The second and third structures have a dipolar resonance on either the carbonyl methyl end, **II_C**, or amide methyl end, **II_N**, and contribute almost equally. Furthermore, the relative contributions of the three leading forms are near the expected ratio of 2:1:1.

For AD_{7eq}, the weight changes associated with methyl group rotation are similar to those observed for the other systems; a nearly 1% increase in **I** for Me_C and 0.5% decrease in **I** for Me_N. Notice, however, that changes in **II_N** occur with Me_C rotation and changes in **II_C** with Me_N rotation. In addition, the weight changes in **IV** are influenced by the motions of both rotors. Structure **IV** complicates the interpretation since contributions from **II_C** or **II_N** appear in two or more structures. To force changes to occur entirely on **I**, **II_N**, and **II_C**, a higher threshold value of 150 kcal/mol was needed. The absolute weights reported in Table 5 still appear in the ratio of 2:1:1. However, the changes associated with **II** are now local to the methyl group. As a result of the additive nature of the changes from the deleted structures, the magnitudes increase by nearly 2-fold for both rotors. We now find that Me_C in the saddle point region affects an increase of more than 2% in **I** and a near commensurate decrease in **II_C**, with little change in the weight of the **II_N** results. Likewise, for the Me_N rotor, the decrease of 0.76% in **I** is largely offset by an increase in **II_N** with little change in **II_C**.

The results for PD_{ICd} also given in Table 5 are similar except that the alternate secondary structures (not shown) gain in importance, decreasing the contributions of **I–IV** by a few percent in some cases. A second distinction occurs as a result

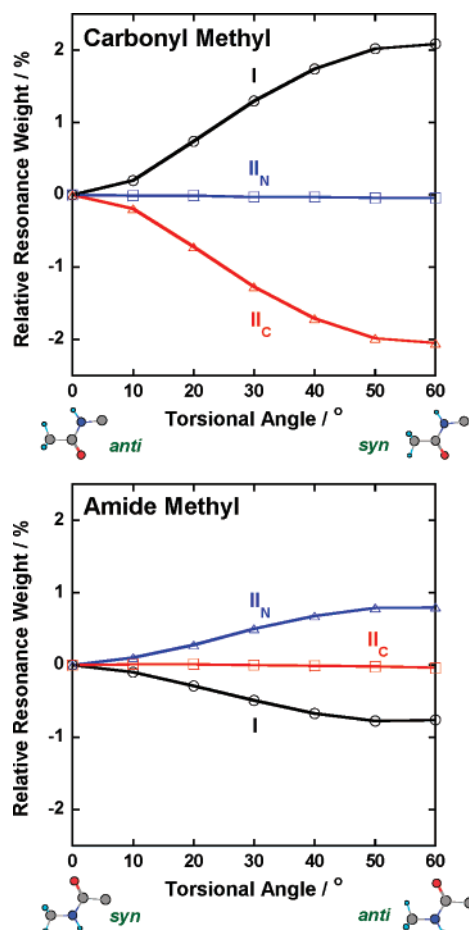


Figure 4. Methyl torsional coordinate dependence of the resonance weights associated with the two peptide bonds of alanine dipeptide (AD_{7eq}) obtained using natural resonance theory with a detection threshold level of 150 kcal/mol. The weight changes in **I**, **II_C** (Me_C end), and **II_N** (Me_N end) are specified relative to the equilibrium values of the Me_C (upper panel) and Me_N (lower panel) rotors of AD_{7eq} .

of the minimum energy *syn* configuration of the Me_C group, reversing the relative importance of **I** and **II** in the saddle point region compared to AD_{7eq} . The magnitudes of the changes are similar suggesting that increased steric interactions of PD_{ICd} have little effect on the resonance weights.

Figure 4 summarizes some of these results in the form of plots of the methyl torsional coordinate dependence of the resonance weights associated with the two peptide bonds in AD_{7eq} . It is immediately apparent that rotation of the carbonyl methyl group from the *anti* to the *syn* position increases the contribution of structure **I** and decreases the contribution of structure **II_C**; concomitantly, rotation of the amide methyl group decreases the contribution of structure **I** and increases the contribution of structure **II_N**. Nuclear motion influences the electronic structure of the molecule.

Further evidence supporting this point of view is revealed by the data in Figure 5. Plotted there are the relative resonance weights of structure **I** as a function of the observed V_3 barriers for all methyl rotors (except Me_C of PD_{ICd}). A clear correlation exists between the experimentally measured torsional barrier heights and the calculated resonance weights of Lewis structure **I**. Nearly equal but opposite changes occur in the weights of Lewis structure **II**. The degree of electronic delocalization is intimately linked to the amplitude of nuclear motion. Larger amplitude motions of the attached methyl groups, a consequence of smaller torsional barriers, result in more equal contributions of the two principal Lewis structures to the peptide bond,

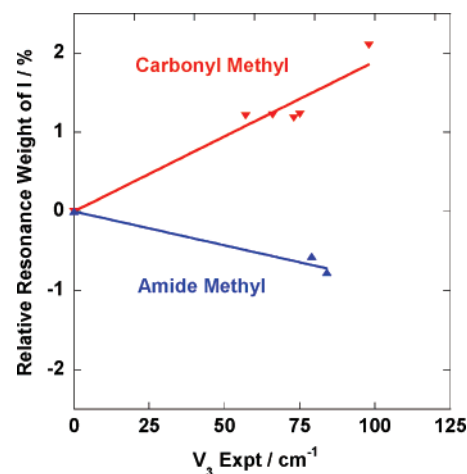


Figure 5. Observed correlation between the experimentally determined V_3 barriers and the resonance weights of the peptide bond of Lewis structure **I** for all rotors except for Me_C of PD_{ICd} . Nearly equal but opposite changes occur in the weights of Lewis structure **II**.

whereas restriction of torsional motion by higher barriers localizes charge and results in less equal contributions of the two structures.

It is well-known that methyl C–H bonds tend to orient themselves *syn* to double bonds in molecules like propene and acetaldehyde; thus, it is not surprising that double-bond character should be influenced by C–H bond orientation.³⁰ The origin of this effect is steric and hyperconjugative in nature; the three hydrogen 1s orbitals of the methyl group can be combined to form three orthogonal “ H_3 ” group orbitals; one of these is used to form a single C– H_3 bond, while the others can overlap with the remaining carbon 2p orbitals. Motion of the methyl group about its torsional axis modulates this hyperconjugative interaction and influences the relative weights of the two principal resonance structures in the peptide bond.

VI. Summary and Conclusions

A new degree of freedom associated with the torsional motion of methyl groups attached α to peptide bonds is found to influence their electronic structure. Natural bond orbital and natural resonance analyses of the HF/6-311++G(d,p) wave functions of five gas-phase biomimetics show that non-Lewis energy differences between the top-of-the-barrier and equilibrium configurations are found to always favor the *anti* configuration of the attached methyl group, whereas Lewis interactions always favor the *syn* configuration. The methyl groups examined fall into two classes; six are attached to the carbonyl end (Me_C) of the peptide bond and three are attached to the amide end (Me_N). For Me_C groups, NLEs are dominant and *anti* minima are preferred. For Me_N rotors, local steric interactions remain important and, consequently, overcome the opposing NLE contributions to give *syn* minima.

The principal NLE contribution for all nine tops involves $n_N \rightarrow \pi_{C=O}^*$ delocalization. This delocalization also defines the relative importance of Lewis structure **II**. Methyl torsional motions affect changes in the NLEs through indirect mechanisms, principally a coupling of vicinal $\sigma \rightarrow \sigma^*$ orbital interactions with the $n \rightarrow \pi^*$, induce shifts in the natural charges, and consequently, modulate the relative weights of Lewis structures **I** and **II** by 0.5%–2%. In most cases, these weight changes are found to correlate with the observed barrier heights; the relative importance of Lewis structure **I** increases (decreases) in Me_C (Me_N) groups having higher barriers. Thus, values of

the barrier heights to internal rotation of methyl groups attached to peptide bonds provide new insights into their electronic structure.

Acknowledgment. Partial financial support of this work was provided by NSF (D.W.P., Grant CHE-0315584).

Supporting Information Available: Correlation diagrams of NBO energies, contour plots of filled and unfilled NBOs, Lewis and non-Lewis energy differences, non-Lewis interaction energies, natural charges of the O, C, and N fragments of the peptide bond, torsional barriers, and resonance weights of principal Lewis structures at the B3LYP and MP2 levels of theory. This material is available free of charge via the Internet at <http://pubs.acs.org>.

References and Notes

- (1) Pauling, L. *The Nature of the Chemical Bond*; Cornell University Press: Ithaca, NY, 1939 and 1960.
- (2) Hirota, E.; Sugisaki, R.; Nielson, C. Y.; Sorensen, G. O. *J. Mol. Spectrosc.* **1974**, *49*, 251.
- (3) (a) Kitano, M.; Kuchitsu, K. *Bull. Chem. Soc. Jpn.* **1974**, *47*, 67. (b) Kitano, M.; Kuchitsu, K. *Bull. Chem. Soc. Jpn.* **1974**, *47*, 631. (c) Kitano, M.; Kuchitsu, K. *Bull. Chem. Soc. Jpn.* **1973**, *46*, 3048.
- (4) Kurland, R. J.; Wilson, E. B. *J. Chem. Phys.* **1957**, *27*, 585.
- (5) (a) Costain, C. C.; Dowling, J. M. *J. Chem. Phys.* **1960**, *32*, 158. (b) Bates, W. W.; Hobbs, M. E. *J. Am. Chem. Soc.* **1951**, *73*, 2151.
- (6) (a) Phillips, W. E. *J. Chem. Phys.* **1955**, *23*, 1363. (b) Stewart, L. M.; Siddal, T. H. *Chem. Rev.* **1970**, *70*, 517. (c) Jackman, L. M.; Cotton, F. A. *Dynamic Nuclear Magnetic Resonance Spectroscopy*; Academic: New York, 1975.
- (7) Allen, F. H.; Kennard, O.; Taylor, R. *Acc. Chem. Res.* **1983**, *16*, 146. (b) Chakrabarti, P.; Dunitz, J. D. *Helv. Chim. Acta* **1982**, *65*, 1547.
- (8) Esposito, L.; Vitagliano, L.; Zagari, A.; Mazzarella, L. *Protein Eng.* **2000**, *13*, 825.
- (9) Rick, S. W.; Cachau, R. E. *J. Chem. Phys.* **2000**, *112*, 5230.
- (10) Mo, Y.; von Rague Schleyer, P.; Wu, W.; Lin, M.; Zhang, Q.; Gao, J. *J. Phys. Chem. A* **2003**, *107*, 10011.
- (11) (a) Wiberg, K. B.; Laidig, K. E. *J. Am. Chem. Soc.* **1987**, *109*, 5935. (b) Wiberg, K. B.; Breneman, C. M. *J. Am. Chem. Soc.* **1992**, *114*, 841. (c) Wiberg, K. B.; Hadad, C. M.; Rablen, P. R.; Cioslowski, J. *J. Am. Chem. Soc.* **1992**, *114*, 8644. (d) Wiberg, K. B.; Rablen, P. R. *J. Am. Chem. Soc.* **1993**, *115*, 9234. (e) Wiberg, K. B.; Rablen, P. R. *J. Am. Chem. Soc.* **1995**, *117*, 2201.
- (12) (a) Laidig, K. E.; Cameron, L. M. *Can. J. Chem.* **1993**, *71*, 872. (b) Laidig, K. E.; Cameron, L. M. *J. Am. Chem. Soc.* **1996**, *118*, 1737.
- (13) Fogarasi, G.; Szalay, P. G. *J. Phys. Chem. A* **1997**, *101*, 1400.
- (14) Knight, E. T.; Allen, L. C. *J. Am. Chem. Soc.* **1995**, *117*, 4401.
- (15) Glendening, E. D.; Hrabal, J. A., II. *J. Am. Chem. Soc.*, **1997**, *119*, 12940.
- (16) Ramachandran, G. N.; Kartha, G. *Nature* **1955**, *176*, 593.
- (17) Frisch, M. J.; Trucks, G. W.; Schlegel, H. B.; Scuseria, G. E.; Robb, M. A.; Cheeseman, J. R.; Montgomery, J. A., Jr.; Vreven, T.; Kudin, K. N.; Burant, J. C.; Millam, J. M.; Iyengar, S. S.; Tomasi, J.; Barone, V.; Mennucci, B.; Cossi, M.; Scalmani, G.; Rega, N.; Petersson, G. A.; Nakatsuji, H.; Hada, M.; Ehara, M.; Toyota, K.; Fukuda, R.; Hasegawa, J.; Ishida, M.; Nakajima, T.; Honda, Y.; Kitao, O.; Nakai, H.; Klene, M.; Li, X.; Knox, J. E.; Hratchian, H. P.; Cross, J. B.; Adamo, C.; Jaramillo, J.; Gomperts, R.; Stratmann, R. E.; Yazyev, O.; Austin, A. J.; Cammi, R.; Pomelli, C.; Ochterski, J. W.; Ayala, P. Y.; Morokuma, K.; Voth, G. A.; Salvador, P.; Dannenberg, J. J.; Zakrzewski, V. G.; Dapprich, S.; Daniels, A. D.; Strain, M. C.; Farkas, O.; Malick, D. K.; Rabuck, A. D.; Raghavachari, K.; Foresman, J. B.; Ortiz, J. V.; Cui, Q.; Baboul, A. G.; Clifford, S.; Cioslowski, J.; Stefanov, B. B.; Liu, G.; Liashenko, A.; Piskorz, P.; Komaromi, I.; Martin, R. L.; Fox, D. J.; Keith, T.; Al-Laham, M. A.; Peng, C. Y.; Nanayakkara, A.; Challacombe, M.; Gill, P. M. W.; Johnson, B.; Chen, W.; Wong, M. W.; Gonzalez, C.; Pople, J. A. *Gaussian 03*, revision C.01; Gaussian, Inc.: Wallingford, CT, 2004.
- (18) (a) Xu, L.-H.; Lees, R. M.; Hougen, J. T. *J. Chem. Phys.* **1999**, *110*, 3835. (b) Xu, L.-H.; Hougen, J. T.; Lees, R. M.; Mekhtiev, M. A. *J. Mol. Spectrosc.* **2002**, *214*, 175. (c) Szalay, V.; Császár, A. G.; Senent, M. L. *J. Chem. Phys.* **2002**, *117*, 6489. (d) Allen, W. D.; Bodi, A.; Szalay, V.; Császár, A. G. *J. Chem. Phys.* **2006**, *124*, 224310.
- (19) (a) Foster, J. P.; Weinhold, F. *J. Am. Chem. Soc.* **1980**, *102*, 7211. (b) Reed, A. E.; Curtiss, L. A.; Weinhold, F. *Chem. Rev.* **1988**, *88*, 899.
- (20) NPA: Reed, A. E.; Weinstock, R. B.; Weinhold, F. *J. Chem. Phys.* **1985**, *83*, 735. NPA is implemented in L607 (NBO 3.1) of the Gaussian program.
- (21) NRT: (a) Glendening, E. D. Ph.D. Thesis, University of Wisconsin, Madison, WI, 1991. (b) Glendening, E. D.; Weinhold, F. *J. Comput. Chem.* **1998**, *19*, 593. NRT is implemented in version 4.0 and 5.0 of the NBO program.
- (22) (a) Glendening, E. D.; Badenhoop, J. K.; Reed, A. E.; Carpenter, J. E.; Bohmann, J. A.; Morales, C. M.; Weinhold, F. *NBO 5.0*; Theoretical Chemistry Institute: Madison, WI, 2001. (b) Weinhold, F. *NBO 5.0 Program Manual*; Theoretical Chemistry Institute: Madison, WI, 2001.
- (23) Ohashi, N.; Hougen, J. T.; Suenram, R. D.; Lovas, F. J.; Kawashima, Y.; Fujitake, M.; Pyka, J. *J. Mol. Spectrosc.* **2004**, *227*, 28.
- (24) Lovas, F. J.; Lavrich, R. J.; Plusquellic, D. F. *J. Mol. Spectrosc.* **2004**, *228*, 251.
- (25) Lavrich, R. J.; Hight Walker, A. R.; Plusquellic, D. F.; Kleiner, I.; Suenram, R. D.; Hougen, J. T.; Fraser, G. T. *J. Chem. Phys.* **2003**, *119*, 5497.
- (26) Lavrich, R. J.; Plusquellic, D. F.; Suenram, R. D.; Fraser, G. T.; Hight Walker, A. R.; Tubergen, M. J. *J. Chem. Phys.* **2003**, *118*, 1253.
- (27) Lavrich, R. J.; Plusquellic, D. F.; Suenram, R. D.; Fraser, G. T.; Hight Walker, A. R.; Tubergen, M. J. *J. Chem. Phys.*, in preparation.
- (28) Plusquellic, D. F.; Kleiner, I.; Demaison, J.; Suenram, R. D.; Lavrich, R. J.; Lovas, F. J.; Fraser, G. T.; Ilyushin, V. V. *J. Chem. Phys.* **2006**, *125*, 104312.
- (29) Kawashima, Y.; Usami, T.; Ohashi, N.; Suenram, R. D.; Hougen, J. T.; Hirota, E. *Acc. Chem. Res.* **2006**, *39*, 216.
- (30) Dorigo, A.; Pratt, D. W.; Houk, K. N. *J. Am. Chem. Soc.* **1987**, *109*, 6591.
- (31) (a) Lii, J.-H.; Allinger, N. L. *J. Comput. Chem.* **1998**, *19*, 1001. (b) Lii, J.-H.; Allinger, N. L. *J. Comput. Chem.* **1991**, *12*, 186. (c) Weiner, S. J.; Kollman, P. A.; Nguyen, D. T.; Case, D. A. *J. Comput. Chem.* **1986**, *7*, 230.
- (32) (a) Brooks, B. R.; Brucoleri, R. E.; Olafson, B. D.; States, D. J.; Swaminathan, S.; Karplus, M. *J. Comput. Chem.* **1983**, *4*, 187. (b) MacKerell, A. D.; Bashford, D.; Bellott, M.; Dunbrack, R. L.; Evaseck, J. D.; Field, M. J.; Fischer, S.; Gao, J.; Guo, H.; Ha, S.; McCarthy, J. D.; Kucnir, L.; Kuczera, K.; Lau, F. T. K.; Mattos, C.; Michnick, S.; Ngo, T.; Nguyen, D. T.; Prohom, B.; Reiher, W. E.; Roux, B.; Schlenkrich, M.; Smith, J. C.; Stote, R.; Straub, J.; Watanabe, M.; Kuczera, W. J.; Yin, D.; Karplus, M. *J. Phys. Chem. B* **1998**, *102*, 3586.
- (33) Ilyushin, V. V.; Alekseev, E. A.; Dyubko, S. F.; Motiyenko, R. A.; Hougen, J. T. *J. Mol. Spectrosc.* **2005**, *229*, 170.